catalysts

MDPI

Article

Study of the Hydrogen Evolution Reaction Using Ionic Liquid/Cobalt Porphyrin Systems as Electro and Photoelectrocatalysts

Leyla Gidi [1], Jessica Honores [1], José Ibarra [1], Roxana Arce [2], M. J Aguirre [3] and Galo Ramírez [1,*]

1 Departamento de Química Inorgánica, Facultad de Química y de Farmacia, Pontificia Universidad Católica de Chile, Av. Vicuña Mackenna 4860, Casilla 306, Correo 22, Santiago 7820436, Chile; ldgidi@uc.cl (L.G.); jshonores@uc.cl (J.H.); jfibarra@uc.cl (J.I.)

2 Departamento de Ciencias Químicas, Facultad de Ciencias Exactas, Universidad Andrés Bello, Av. República 275, Santiago 8370186, Chile; roxana.arce@unab.cl

3 Departamento de Química de los Materiales, Facultad de Química y Biología, Universidad de Santiago de Chile USACH. Av. L.B. O'Higgins 3363, Santiago 9170019, Chile; maria.aguirre@usach.cl

* Correspondence: gramirezj@uc.cl

Received: 8 January 2020; Accepted: 22 January 2020; Published: 17 February 2020

Abstract: In this work, the design and manufacture of graphite paste (Gr) electrodes is carried out, including *N*-octylpyridinium hexafluorophosphate ($OPyPF_6$) ionic liquid (IL) as binder and modification with Co-octaethylporphyrin (Co), in order to study the hydrogen evolution reaction (HER) in the absence and presence of light. The system is characterized by XRD and FESEM-EDX (Field Emission Scanning Electron Microscopy with Energy Dispersive X-Ray Spectroscopy), confirming the presence of all the components of the system in the electrode surface. The studies carried out in this investigation confirm that a photoelectrocatalytic system towards HER is obtained. The system is stable, efficient and easy to prepare. Through cyclic voltammetry and electrochemical impedance spectroscopy, was determined that these electrodes improve their electrochemical and electrical properties upon the addition of $OPyPF_6$. These effects improve even more when the systems are modified with Co porphyrin. It is also observed that when the systems are irradiated at 395 nm, the redox process is favored in energy terms, as well as in its electrical properties. Through gas chromatography, it was determined that the graphite paste electrode in the presence of ionic liquid and porphyrin (Gr/IL/Co) presents a high turnover number (TON) value (6342 and 6827 in presence of light) in comparison to similar systems reported.

Keywords: hydrogen evolution reaction; photoelectrocatalysis; ionic liquids; metalloporphyrins

1. Introduction

Hydrogen evolution reaction (HER) corresponds to the generation of hydrogen gas from water electrolysis. This reaction has been widely studied because of its potential use as fuel in the production of clean and sustainable energy [1,2]. Electrodes manufactured with carbonaceous materials [3,4] have been designed to electrocatalyze this reaction, for instance in the case of carbon paste electrodes [5,6]. These electrodes can include other components in order to improve their electrochemical and electrical properties.

These components can include ionic liquids (IL), which are attractive materials since they can be used as binders on paste electrodes, increasing current values compared to the use of other conventional binders (mineral oil or paraffin) [7]. They have also shown important advantages according to their physicochemical properties that allow their use in green chemistry [8]. The ionic liquids based on

N-octylpyridinium ($OPyPF_6$) show favorable responses towards electrochemical reactions of interest when studied in paste electrodes [9–11].

Porphyrins are azo-macrocyclic complexes composed of a system of pyrrole rings with aromatic character that can be coordinated with a transition metal [12]. Metalloporphyrins can be used to modify electrodes, since they have an interesting redox activity and stand out for their high electrocatalytic performance towards electrochemical reactions such as HER [13–15]. Moreover, when irradiated at determined wavelengths, they can become photocatalysts [16,17] due to the electronic transition from HOMO to LUMO. Exited species present a very labile electron while an electronic vacancy (h^+) is produced. In this way, both reduction and oxidation processes are photocatalyzed [18]. In previous works, it was determined that Co (II) and Cu (II) octaethylporphyrins deposited on glassy carbon are capable of catalyzing HER [14], becoming even more efficient when they are in the presence of light [15].

Based on the aforementioned information, graphite paste electrodes bound with ionic liquid $OPyPF_6$ and their modification with Co (II) octaethylporphyrins are manufactured in order to study the electro and photoelectrocatalytic effect of these systems towards HER. Characterization of the material obtained was also performed using XRD and FESEM-EDX. Finally, the quantification of produced H_2 was performed through gas chromatography.

2. Results and Discussion

2.1. Crystallographic Characterization

The different systems, graphite and the incorporation of Co porphyrin and IL are studied by XRD. Figure 1a shows the signals corresponding to the crystal phases of graphite powder with a signal at 2θ = 26.383° associated to the plane C(002), typical of graphite materials. This peak indicates the presence of a hexagonal structure typical of carbonaceous materials [19]. In Figure 1b, the signals of IL are shown, accounting for a high crystallinity since the diffraction peaks are narrow and intense compared to the baseline. For the Co porphyrin sample in Figure 1c, there is low crystallinity reflected on the noise and the low intensity of the diffraction peaks. In Figure 1d, corresponding to the graphite paste/ionic liquid (Gr/IL) system, typical graphite signals were observed, with higher intensity than the signals of the ionic liquid observed between 20 and 30°. On the other hand, the system Gr/IL/Co (Figure 1e) shows a diffractogram like the one of Gr/IL. Given the low crystallinity of the Co porphyrin, it was not possible to observe the diffraction peaks. Finally, in Figure 1f the comparison of the diagrams of Gr, Gr/IL and GR/IL/Co is presented. The inserted figure corresponds to an approximation between 24 and 28° of the signal associated to plane C(002). Here, it can be noted that the intensity of the signals was different for each case, diminishing when IL and Co were present. For the Gr/IL and Gr/IL/Co systems, the signal moves to the right, centering at 26.400° and 26.429° respectively. This is due to the tension on the material in which the distances within the unit cell vary in size. In this case, as the movement of the signal occurred to higher angles, the tension comprised of the unit cell, therefore decreasing the values in the lattice parameter values [20].

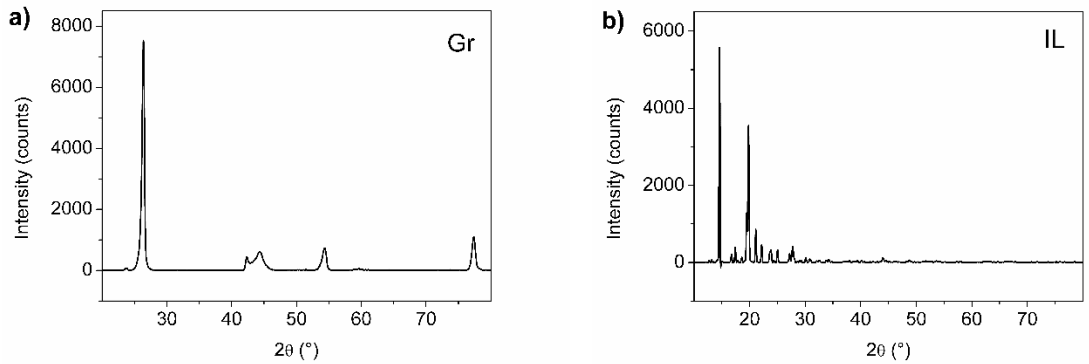

Figure 1. *Cont.*

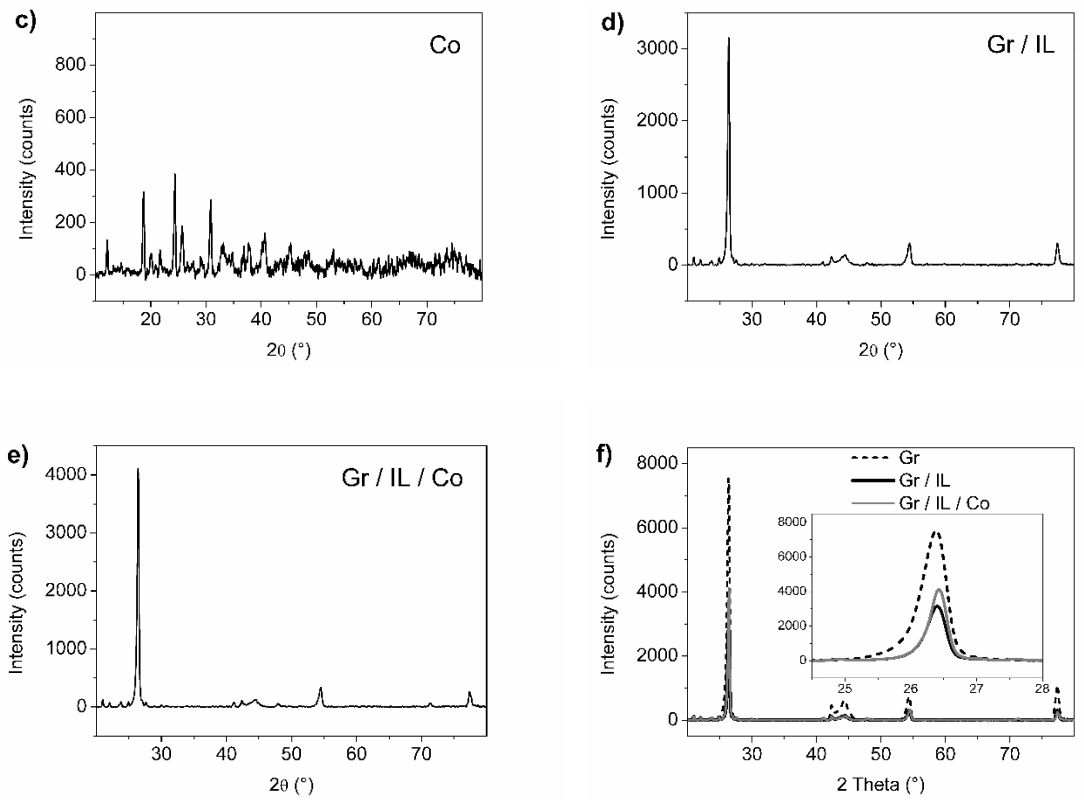

Figure 1. Diffractograms for the graphite paste/ionic liquid (Gr/IL) and Gr/IL/Co systems and their components. (**a**) Graphite powder, (**b**) IL $OPyPF_6$ (**c**) cobalt (II) 2,3,7,8,12,13,17,18-octaethyl-21H,23H-porphine, (**d**) system Gr/IL (**e**) system Gr/IL/Co and (**f**) systems comparison.

2.2. Morphological Characterization

The FESEM images (Figure 2) show the surface of graphite pastes that include mineral oil (Gr), ionic liquid (Gr/IL) and both the ionic liquid and the Co porphyrin (Gr/IL/Co). All the surfaces are significantly different: in the case of the systems Gr and Gr/IL, the type of agglutination varies because of the change of binder when using IL instead of mineral oil. When adding Co porphyrin, generating the Gr/IL/Co system, long fiber-shaped structures can be observed, which are typical for this type of porphyrin [21].

Through FESEM coupled to an X-ray microanalyzer (FESEM-EDX), the chemical composition of the Gr/IL/Co system was studied at a magnification 6525× (Figure 3). The weight percentage values for each element present in the surface are summarized in Table 1. The main percentage belonged to carbon (near 70%), which is expected as the carbon paste contains graphite and IL in 7:3 proportion. Phosphorous and fluorine content was also detected, corresponding to the anion of IL (OPyPF6). Moreover, traces of Co were quantified in this analysis (0.84%). This value was low, because the porphyrin mainly presented carbon atoms in its macrostructure and a Co atom in the center. Additionally, the porphyrin solution quantity used to modify the surface was small (10 µL, 0.2 mM).

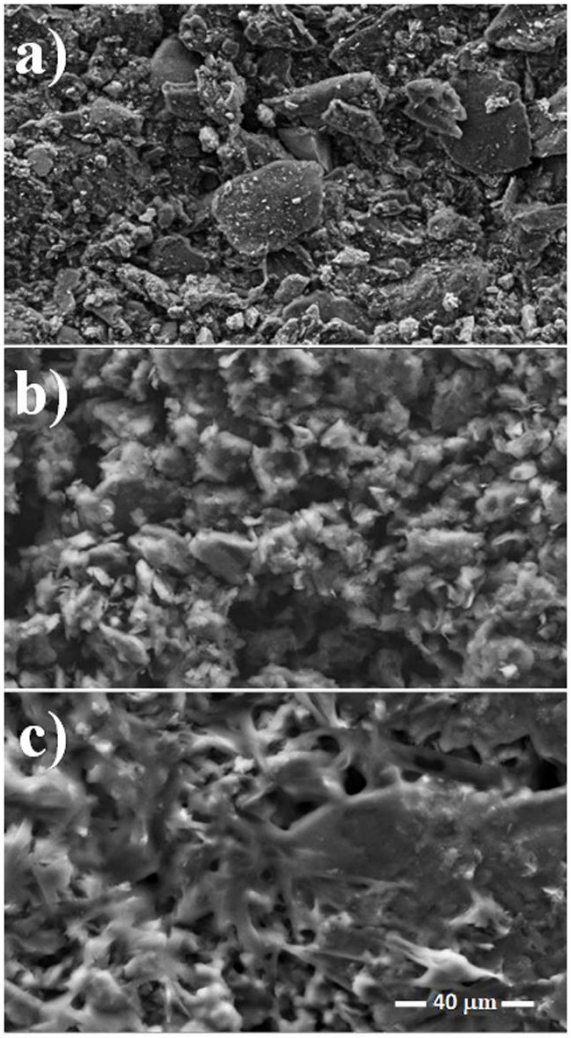

Figure 2. FESEM images for the systems (**a**) Gr, (**b**) Gr/IL and (**c**) Gr/IL/Co. Magnification = 2500×.

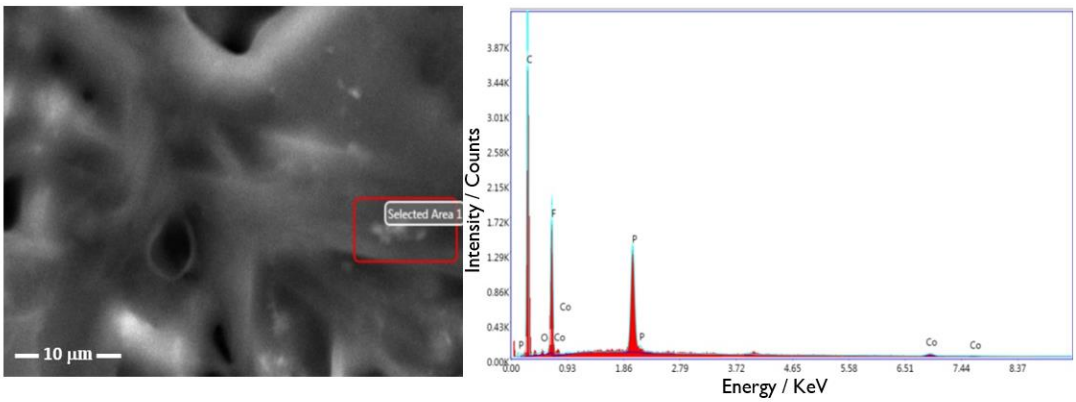

Figure 3. FESEM image and composition study by EDX for the system Gr/IL/Co. Magnification = 6525×.

Table 1. Weight percentage of the elements present in the surface of the system Gr/IL/Co obtained by FESEM-EDX.

Element	Weight Percentage (%)
C	69.65
O	0.77
F	21.56
P	7.19
Co	0.84

2.3. UV-Vis Spectroscopy

Figure 4 shows the absorption spectra of Co porphyrin. The UV-vis spectrum of porphyrins in solution (Figure 4a) shows the Soret band between 350 and 450 nm. This band accounts for an electronic transition to the second excited singlet ($S_0 \rightarrow S_2$) [22] and it is more intense than the Q bands. The later appears between 500 and 700 nm as a result of an electronic transition π–π* to the first excited singlet ($S_0 \rightarrow S_1$) [22].

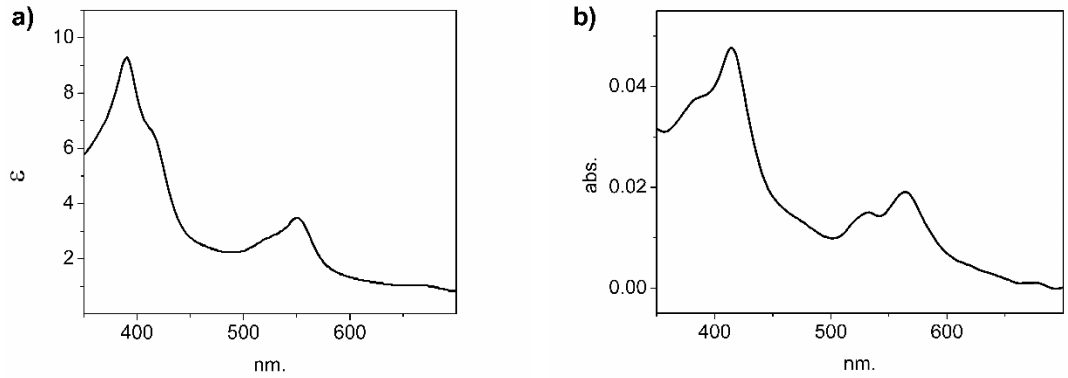

Figure 4. UV-vis spectra (**a**) in solution and (**b**) in solid, of 0.025 mM cobalt octaethylporphyrin in DCM/hexane 2:8.

The UV-vis spectrum in solid (Figure 4b) characterizes the porphyrins deposited on glass as an approximation to the modification on graphite paste. It is interesting to highlight that the Co porphyrin shows variations in the adsorption spectra when in solution and in solid. The unfolding of the Soret band associates to the existence of two types of porphyrin populations: monomers and aggregates. The bathochromic effect of the Soret and Q bands indicates that these aggregates would be J-type or side-by-side [23–25].

2.4. Electrochemical and Electric Characterization

Graphite paste electrodes using mineral oil as a binder and the incorporation of IL (instead of mineral oil) and Co porphyrin were studied towards HER through voltammetric profiles and electrochemical impedance spectroscopy. In Figure 5a, the system Gr/IL/Co shows the highest electrocatalytic activity in terms of potential, followed by Gr/IL, Gr/Co and finally by Gr. This demonstrates that both the IL and the Co porphyrin could catalyze HER due to an enhancement between the materials. The electrode that contains both components (Gr/IL/Co) shows a higher shift towards less negative potentials in comparison to the systems that contain only one component.

Figure 5b shows Nyquist plots for the same systems. When charge transfer resistance Rct is smaller, the systems conduct the electric current better than electrodes with higher Rct [26]. Therefore, low Rct values imply more conductive surfaces. In Figure 5b, the system that shows the lowest Rct was Gr/IL/Co, followed by Gr/IL, Gr/Co and Gr. This result was coherent with the voltammetric

study, establishing for this case a direct relation between catalytic activity and conductive capacity of the electrodes.

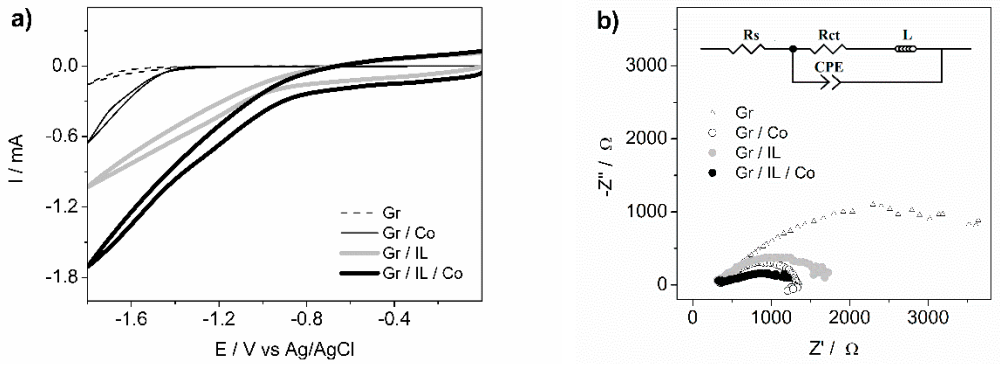

Figure 5. (**a**) Voltammetric profiles and (**b**) Nyquist plot towards a hydrogen evolution reaction (HER) and equivalent circuit used. Phosphate buffer at pH = 7, in Ar saturation. $\Omega = 0.1\ V{\cdot}s^{-1}$.

The equivalent circuit inserted in Figure 5b presents a solution resistance (Rs), a charge transfer resistance (Rct), an inductor (L), because of the generation of intermediary species in the surface, [17,18] and a constant phase element (CPE). These parameters are summarized in Table S1 of supplementary material.

Considering that Gr/IL/Co is the system that presents the higher electrocatalytic activity and knowing that Co porphyrin has the ability to absorb light in the UV-vis range, the study of HER on this modified electrode was performed by cyclic voltammetry and electrochemical impedance spectroscopy in the absence and presence of light. The nine wavelengths presented in Table S2 of supplementary material were used. In previous works, it has been established that the photoelectrocatalytic activity of the metal octaethylporphyrin is independent to the intensity of the lamps, [15] being decisive of the value of the applied wavelength.

Upon irradiating the surface of the modified electrode, a higher effect in terms of electrocatalytic activity (Figure 6a) could be observed, and in terms of its conductive properties (Figure 6b) when a wavelength of 395 nm was used. It is important to mention that this wavelength coincided with the Soret band of the adsorption spectrum of Co porphyrin in Figure 4. As mentioned in a previous work [27], the activity of the catalysts depended on the wavelength applied and not on the intensity of the light. The onset potentials and charge transfer resistance for all the systems in study are summarized in Table 2.

The Gr/IL/Co modified electrode presents a high electrocatalytic activity, which improves when irradiating at 395 nm. This system was selected to determine the HER mechanism through Tafel slope (Figure 7). For similar materials, Tafel slopes close to 160 mV per decade in aqueous solution (pH ≈ 7) have been reported [15,28].

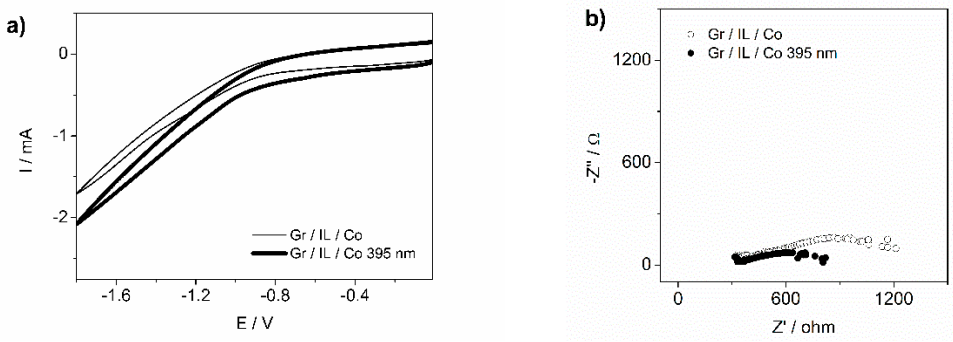

Figure 6. (**a**) Voltammetric profiles and (**b**) Nyquist plot towards HER. Phosphate buffer at pH = 7 in Ar saturation. $\Omega = 0.1\ V{\cdot}s^{-1}$.

Table 2. Onset potential (*E_O) and charge transfer resistance (Rct) values.

System	E_O/V	Rct/Ω
Gr	−1.46	3950
Gr/Co	−1.34	1010
Gr/IL	−0.99	1510
Gr/IL/Co	−0.91	960
Gr/IL/Co 395 nm	−0.89	545

* E_O was determined with respect to the Ag/AgCl reference electrode, considering the potential where the reduction current increase begins.

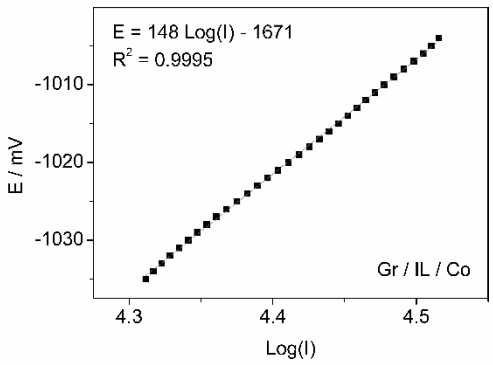

Figure 7. Tafel slope for the Gr/IL/Co system measured in the phosphate buffer pH = 7, Ω = 5 $mV{\cdot}s^{-1}$.

For the Gr/IL/Co system, the Tafel slope is 148 mV per decade. This value is consistent with the Volmer–Heyrovsky mechanism, [23,29,30] according to adsorption and desorption processes presented in Equations (1)–(3). The slow stage would be the Equation (2) [31].

$$M + H_3O^+ + e^- \rightarrow M\text{-}H_{ads} + H_2O, \quad (1)$$

$$M\text{-}H_{ads} + H_3O^+ + e^- \rightarrow M + H_2 + H_2O, \quad (2)$$

$$M\text{-}H_{ads} + M\text{-}H_{ads} \rightarrow H_2 + 2M. \quad (3)$$

This system also has the advantage of being stable, showing relatively constant currents in time for a 2-h period when applying a controlled potential of −1.3 V (Figure S1 of supplementary material).

2.5. Chromatographic Quantification

The quantity of hydrogen produced using the system Gr/IL/Co was determined through electrolysis at a fixed potential of −1.3 V in a two-compartment sealed electrochemical cell. The working electrode (Gr/IL/Co) with an electroactive area of 1.83 cm^2 produces the reduction of protons to gaseous hydrogen in one of these compartments. Another compartment contains a platinum counter electrode where oxygen is produced simultaneously. The generation of both gases (hydrogen and oxygen) is corroborated by the formation of bubbles in both sides of the cell. The electrolysis process is carried out for 2 h, and every 1 h, an injection of 50 µL of gas from the working electrode compartment is obtained to be studied by gas chromatography. The hydrogen concentration (CH) is calculated by performing a calibration curve (Figure S2 of supplementary material), whose linear equation is A = 604.45CH − 21.19; R^2 = 0.991. The values of CH obtained by gas chromatography are in Table 3.

Then, after 2 h of electrolysis, the systems Gr/IL/Co and Gr/IL/Co 395 nm produced 56.5 and 57.3 µmoles of H_2, corresponding to 15.4 and 15.7 $\mu mol{\cdot}h^{-1}{\cdot}cm^{-2}$ respectively using the electroactive area (1.83 cm^2). The turnover number (TON) was calculated through the ratio between the H2 moles determined by gas chromatography and catalyst moles [15]. The amount of catalyst deposited on the electrode was determined considering the relation between the electric current, charge and time of Equation (4) and Faraday's Law of electrolysis (Equation (5)), [32], applied to the voltagramm of

systems Gr/IL/Co and Gr/IL/Co 395 nm employed on the chromatographic determination (Figure S3 of supplementary material). In Equation (4), Q is the charge, I is the magnitude of the faradaic current ($1.91 \cdot 10^{-4}$ and $1.8 \cdot 10^{-4}$ A for the systems in the absence and in the presence of light respectively) and t is time. The time is obtained from the ratio between magnitude of E_O and scan rate (0.1 $V \cdot s^{-1}$), therefore $Q = 1.74 \cdot 10^{-3}$ C for Gr/IL/Co and $1.62 \cdot 10^{-3}$ C for Gr/IL/Co 395 nm.

Table 3. Hydrogen concentration (C_H), amount of catalyst (N) and turnover number (TON) obtained using the systems Gr/IL/Co and Gr/IL/Co 395 nm.

System	C_H/µmol	C_H/µmol h^{-1} cm^{-2}	N/mol	TON
Gr/IL/Co	56.5	15.4	9.01×10^{-9}	6342
Gr/IL/Co 395 nm	57.3	15.7	8.40×10^{-9}	6827

In Equation (5), N is the amount of catalyst deposited on electrode in moles, F is the Faraday constant (96485 C·mol-1), [32] n is the number of electrons involved in the reaction, which in the case of HER are 2. In this way, it is determined the catalyst quantity and the turnover number (Table 3). These values are higher than similar systems previously reported in literature (Table 4).

$$I = \left(\frac{dQ}{dt}\right), \tag{4}$$

$$Q = N \cdot F \cdot n. \tag{5}$$

Table 4. Comparison of onset potential (E_O) and catalyst turnover number (TON) in similar systems.

System	pH	E_O/V Ag/AgCl	E_O/V RHE	TON	Ref.
Commercial Pt/C	7	≈−0.66 *	≈−0.05	-	[33]
$[Co(TPP)](COOH)_4]$	≈7	−0.92	−0.31 *	51.8	[34]
$[Co(TPP)](SO_{43}H)_4]$	≈7	−0.75	−0.14 *	104.1	[34]
$[Co(TPP)](NH_2)_4]$	≈7	−1.01	−0.40 *	46	[34]
$[Co(bpyPY2Me)(CH_3CN)(CF_3SO_3)](CF_3SO_3)]$	≈4	−1.11	−0.50 *	4200	[35]
dinuclear cobalt(II)etriazenido complex	4.6	≈−1.1	≈−0.5 *	4367	[36]
dinuclear cobalt(II)etriazenido complex	7	≈−1.3	≈−0.7 *	4367	[36]
GC + 4AP + Co(II)OEP	≈7	−1.17	−0.56 *	6000	[13]
Gr/IL/Co	7	−0.91	−0.30 *	6342	This work
Gr/IL/Co 395 nm	7	−0.89	−0.28 *	6827	This work

* Transformed values between Ag/AgCl and RHE reference electrodes.

The faradaic efficiency *f(%)* is determined through Equation (6), where C_H is the number of moles of hydrogen produced, n is the number of electrons transferred (2 for the HER), F is 96485 $C \cdot mol^{-1}$ and q is the charge after 2 h of electrolysis obtained from Figure S1. The values of q and *f(%)* are summarized in Table 5. Here, both systems Gr/IL/Co and Gr/IL/Co 395 nm show similar values of *f(%)* (over 50%).

$$f(\%) = \frac{C_H \cdot n \cdot F}{q} \times 100. \tag{6}$$

Table 5. q and *f(%)* values for the systems Gr/IL/Co and Gr/IL/Co 395 nm.

System	*q*/C	*f(%)*
Gr/IL/Co	19.1	57
Gr/IL/Co 395 nm	21.7	51

3. Materials and Methods

3.1. Reagents and Solutions

Potassium chloride, graphite powder, hexane, pyridine, acetonitrile (HPLC grade) diethyl ether and dichloromethane (DCM; analytical grade) were obtained from Merck. Ultra-pure water was obtained from a Millipore-Q system (18.2 MΩcm). Argon (99.99% pure) was purchased from AGA, Chile. Cobalt (II) 2,3,7,8,12,13,17,18-octaethyl-21H,23H-porphine, potassium dihydrogen phosphate, disodium hydrogen phosphate, 1-bromooctane, potassium hexafluorophosphate and mineral oil were all purchased from Sigma-Aldrich Chile.

3.2. Synthesis of the Ionic Liquid

The ionic liquid (IL) synthesis is performed through a method consisting of two stages [37]. The first stage consists of the quaternization of pyridine to obtain OPyBr and the second stage is the anionic interchange to obtain $OPyPF_6$. First, 10 mL of pyridine, 21.5 mL of 1-bromooctane and 20 mL of acetonitrile were refluxed in Ar atmosphere at 100 °C for 48 h. The solvent was evaporated, and the compound was dried at 90 °C for 15 h (yield = 93%). Then, 12.54 g of OPyBr generated in the first step of the reaction was mixed with 8.70 g of KPF_6, 20 mL of DMC and 20 mL of ultra-pure water in a glass flask, and the mixture was stirred at room temperature for 2 h. After washing and extracting the organic phase, the solvent was evaporated and the compound was recrystallized in 95% ethanol, to later be dried at 90 °C for 24 h (yield = 91%). The structure of $OPyPF_6$ was confirmed by spectra characterization ^{1}H NMR, ^{13}C NMR and ^{19}F NMR.

^{1}H NMR (400 MHz, $CDCl_3$) δ 8.63 (d, *J* = 6.1 Hz, 2H, H2 and H6), 8.43 (t, *J* = 7.7 Hz, 1H, H4), 7.97 (t, *J* = 7.0 Hz, 2H, H3 and H5), 4.51 (t, *J* = 7.6 Hz, 2H, 2 × H1′), 1.98−1.84 (m, 2H, 2 × H2′), 1.32−1.15 (m, 10H, 2 × H3′-H7′), 0.82 (t, *J* = 6.6 Hz, 3H, 3 × H8′).

^{13}C NMR (101 MHz, $CDCl_3$) δ 145.64, 144.07 (2C), 128.59 (2C), 62.57, 31.60, 31.36, 28.90, 28.81, 25.96, 22.53, 14.02.

^{19}F NMR (376 MHz, $CDCl_3$) δ −72.23 (d, $^1J_{P\text{-}F}$ = 712.2 Hz, PF_6).

3.3. Electrode Preparation

As reported before [27], powder graphite was mixed with the binder (mineral oil or IL) in a 7:3 proportion in mass in an agate mortar, adding diethyl ether. The mixture was homogenized until the complete evaporation of diethyl ether, obtaining a paste that was used to fill a Teflon hollow electrode, compacting completely. A solution of 0.2 M Co (II) octaethylporphyrin was prepared in DCM/hexane (2:8 proportion). Of porphyrin solution 10 µL was added to the paste electrode surface and let to evaporate at room temperature. After 5 min, the surface of the electrode was carefully washed with ultra-pure water.

3.4. Instrumentation

A Bruker B8 Advance diffractometer was used, operating with a $CuK_{\alpha 1,2}$; K_β X ray tube generated at 30 rmp, 40 kV and 40 mA. The scans were performed with a period of 1.0 and 3.0 s, for values of 2θ between 10 and 80° and 20 and 80° and increase of 0.02°. A scintillation detector was employed.

A scanning electron microscope with a field emission cathode (FE-SEM) coupled to the composition analysis by the energy-dispersive X-ray (EDX) model FEI Quanta^{TM} 250 FEG was also employed.

UV-Vis spectroscopy was performed in UV-2600 UV-VIS SPECTROPHOTOMETER SHIMADZU equipment, with a module to study samples in solution inside a quartz cell, and a second module to analyze solid samples over a glass plate. On the analyses performed on both modules, the porphyrins on DCM/hexane 2:8 was studied. To study the sample (in solid), 0.5 mL of 0.2 mM Co (II) porphyrin solution was deposited over the glass surface and the solvent was dried at room temperature. The spectra were obtained between 350 and 700 nm.

The activity of electrodes was studied in a three-compartment cell. It used an Ag/AgCl reference electrode in 3 M KCl, the working electrode and a platinum counter electrode that contained 0.1 M phosphate buffer (pH = 7), saturated with argon for 20 min.

Voltammetry, electrical impedance spectroscopy (EIS) and chronoamperometry analyses were performed by using a CH Instruments 750D potentiostat. In the characterization by EIS, 100,000 Hz to 1 Hz frequencies and 0.005 V amplitude were used. The measurements were performed in 0.1 M phosphate buffer (pH = 7) bubbled with argon for 20 min at a potential of −1.3 V.

Photoelectrocatalytic studies were carried out within a dark and closed box. It used an electrochemical cell equipped with a quartz window to ensure an adequate irradiation of the surfaces by using a monochromator with nine available lamps between 380 and 660 nm (Table S2 of supplementary material). The distance between the monochromator and the modified electrode was 10 cm.

The quantification of hydrogen gas produced by the manufactured electrode was carried out in a sealed electrolysis cell in which HER was performed at the working electrode compartment at a fixed potential of −1.3 V. The compartments were separated by a salt bridge filled with agar at 2.5% m/V in KCl 1 M. While the electrocatalysis occurred, the phosphate buffer solution at pH = 7 (in Ar saturation) was agitated to favor the hydrogen bubbles rise to the Head Space of the cell. Every 1 h 50 μL of gas was obtained and analyzed by gas chromatography in a DANI-Instruments® Gas Chromatograph.

4. Conclusions

In this work, a graphite paste electrode modified with the addition of OPyPF6 as a binder and Co porphyrin was obtained, in order to study HER. The study through XRD shows the presence of the components of the system and indicates that both the IL and the Co porphyrin generated a compression effect on the graphite unit cell. By FESEM, it was observed that the surfaces of the systems were evidently different and by FESEM-EDX the presence of IL (PF_6^-) anion and Co coming from the porphyrin on the surface of the Gr/IL/Co electrode were corroborated. It was determined that the Gr/IL/Co system was the electrode that shows a higher electrocatalytical effect and lower charge transfer resistance towards this reaction in comparison to the other systems. These properties improved even more when the system was irradiated at 395 nm, accounting for its photoelectrocatalytic ability. It is determined that, when using this system, HER occurred through the Volmer–Heyrovsky mechanism. Finally, in accordance to the chromatographic studies, the electrode shows a high TON value (6342 in absence and 6827 in presence of light) in relation to the use of similar systems reported in literature and a faradaic efficiency over 50%.

Supplementary Materials: The following are available online at http://www.mdpi.com/2073-4344/10/2/239/s1, Figure S1: Study of current stability in electrolysis time at −1.3 V, for 2 h for the system Gr/IL/Co. Phosphate buffer at pH = 7. Figure S2: Linear relation between area and hydrogen concentration obtained by gas chromatography using extra pure hydrogen (99.999%), Figure S3: Voltammetric profile of the Gr/IL/Co and Gr/IL/Co 395 nm systems used in the chromatographic determination. Phosphate buffer at pH = 7 in Ar saturation. $\upsilon = 0.1\ V{\cdot}s^{-1}$, Table S1: Wavelenght (λ) and intensity of the lamps used in the study, Table S2: Parameters obtained for the electrodic systems towards HER. Rs is the solution resistance, Rct is the charge transfer resistance, L is inductance and CPE is the constant phase element.

Author Contributions: L.G. and J.H. performed the experiments. J.I. and R.A. investigated the relevant literature and helped to write this manuscript. M.J.A. Aguirre and G.R., wrote, reviewed and modified this manuscript. All authors have read and agreed to the published version of the manuscript.

Funding: This research received no external funding.

Acknowledgments: This work was supported by FONDECYT Project number 1170340; FONDECYT Project No. 1160324; Dicyt-Usach and Doctoral Scholarship CONICYT Project No. 21170542; FONDECYT postdoctorado No: 3180061.

Conflicts of Interest: The authors declare no conflict of interest.

References

1. Hanley, E.S.; Deane, J.P.; Gallachóir, B. The role of hydrogen in low carbon energy futures—A review of existing perspectives. *Renew. Sustain. Energy Rev.* **2018**, *82*, 3027–3045. [CrossRef]
2. Rong, J.; Xu, J.; Qiu, F.; Zhu, Y.; Fang, Y.; Xu, J.; Zhang, T. Sea Urchin-Like MOF-Derived Formation of Porous Cu_3P@C as an Efficient and Stable Electrocatalyst for Oxygen Evolution and Hydrogen Evolution Reactions. *Adv. Mater. Interfaces* **2019**, *6*, 1900502. [CrossRef]
3. Sengupta, R.; Bhattacharya, M.; Bandyopadhyay, S.; Bhowmick, A.K. A review on the mechanical and electrical properties of graphite and modified graphite reinforced polymer composites. *Prog. Polym. Sci.* **2011**, *36*, 638–670. [CrossRef]
4. Thornton, D.C.; Corby, K.T.; Spendel, V.A.; Jordan, J.; Robbat, A.; Rutstrom, D.J.; Gross, M.; Ritzler, G. Pretreatment and validation procedure for glassy carbon voltammetric indicator electrodes. *Anal. Chem.* **1985**, *57*, 150–155. [CrossRef]
5. Munoz, J.; Baeza, M. Customized bio-functionalization of nanocomposite carbon paste electrodes for electrochemical sensing: A mini review. *Electroanalysis* **2017**, *29*, 1660–1669. [CrossRef]
6. Kalcher, K. Chemically modified carbon paste electrodes in voltammetric analysis. *Electroanalysis* **1990**, *2*, 419–433. [CrossRef]
7. Shvedene, N.V.; Chernyshov, D.V.; Pletnev, I.V. Ionic liquids in electrochemical sensors. *Russ. J. Gen. Chem.* **2008**, *78*, 2507–2520. [CrossRef]
8. Abo-Hamad, A.; AlSaadi, M.A.; Hayyan, M.; Juneidi, I.; Hashim, M.A. Ionic Liquid-Carbon Nanomaterial Hybrids for Electrochemical Sensor Applications: A Review. *Electrochim. Acta* **2016**, *193*, 321–343. [CrossRef]
9. Momeni, S.; Farrokhnia, M.; Karimi, S.; Nabipour, I. Copper hydroxide nanostructure-modified carbon ionic liquid electrode as an efficient voltammetric sensor for detection of metformin: A theoretical and experimental study. *J. Iran. Chem. Soc.* **2016**, *13*, 1027–1035. [CrossRef]
10. Momeni, S.; Nabipour, S.I. A simple green synthesis of palladium nanoparticles with Sargassum alga and their electrocatalytic activities towards hydrogen peroxide. *Appl. Biochem. Biotechnol.* **2015**, *176*, 1937–1949. [CrossRef]
11. Eslami, E.; Farjami, F. Electrochemical determination of amitriptyline using a nanocomposite carbon paste electrode in human body fluids. *Phys. Chem. Electrochem.* **2016**, *4*, 111–117.
12. Hoard, J.L.; Smith, K.M. *Porphyrins and Metalloporphyrin*; Elsevier: Amsterdam, The Netherlands, 1975.
13. Bodedla, G.B.; Li, L.; Che, Y.; Jiang, Y.; Huang, J.; Zhao, J.; Zhu, X. Enhancing photocatalytic hydrogen evolution by intramolecular energy transfer in naphthalimide conjugated porphyrins. *Chem. Commun.* **2018**, *54*, 11614–11617. [CrossRef]
14. Canales, C.; Varas-Concha, F.; Mallouk, T.E.; Ramírez, G. Enhanced electrocatalytic hydrogen evolution reaction: Supramolecular assemblies of metalloporphyrins on glassy carbon electrodes. *Appl. Catal. B: Environ.* **2016**, *188*, 169–176. [CrossRef]
15. Canales, C.; Olea, A.F.; Gidi, L.; Arce, R.; Ramírez, G. Enhanced light-induced hydrogen evolution reaction by supramolecular systems of cobalt (II) and copper(II) octaethylporphyrins on glassy carbon electrodes. *Electrochim. Acta* **2017**, *258*, 850–857. [CrossRef]
16. Ladomenou, K.; Natali, M.; Iengo, E.; Charalampidis, G.; Scandola, F.; Coutsolelos, A.G. Photochemical hydrogen generation with porphyrin-based systems. *Coord. Chem. Rev.* **2015**, *304*, 38–54. [CrossRef]
17. Natali, M.; Luisa, A.; Iengo, E.; Scandola, F. Efficient photocatalytic hydrogen generation from water by a cationic cobalt (II) porphyrin. *Chem. Commun.* **2014**, *50*, 1842–1844. [CrossRef] [PubMed]
18. Ramirez, G.; Ferraudi, G.; Chen, Y.Y.; Trollund, E.; Villagra, D. Enhanced photoelectrochemical catalysis of CO_2 reduction mediated by a supramolecular electrode of packed CoII (tetrabenzoporphyrin). *Inorg. Acta* **2009**, *362*, 5–10. [CrossRef]
19. Moore, D.M.; Reynolds, R.C. *X-ray Diffraction and the Identification and Analysis of Clay Minerals*; Oxford University Press: New York, NY, USA, 1989; Volume 332.
20. Hauk, V.M.; Macherauch, E. A Useful Guide for X-ray Stress Evaluation (XSE). *Adv. X-ray Anal.* **1984**, *27*, 81–99.
21. Canales, C.; Gidi, L.; Arce, R.; Armijo, F.; Aguirre, M.J.; Ramírez, G. Electro-Reduction of Molecular Oxygen Mediated by a Cobalt (II)octaethylporphyrin System onto Oxidized Glassy Carbon/Oxidized Graphene Substrat. *Catalysts* **2018**, *8*, 629. [CrossRef]
22. Josefsen, L.B.; Ross, W.B. Photodynamic therapy and the development of metal-based photosensitisers. *Met. Based Drugs* **2008**, *2008*, 276109. [CrossRef]

23. Lasia, A.; Rami, A. Kinetics of hydrogen evolution on nickel electrodes. *Electroanal. Chem.* **1990**, *294*, 123–141. [CrossRef]
24. Frumkin, A.N. Hydrogen overvoltage and adsorption phenomena. In *Advances in Electrochemistry and Electrochemical Engineering*; Delahay, P., Tobias, C.W., Eds.; Interscience Publishers Inc: New York, NY, USA, 1963; Volume 3, pp. 65–122.
25. Bernhardt, P.V.; Jones, L.A. Electrochemistry of Macrocyclic Cobalt (III/II) Hexaamines: Electrocatalytic Hydrogen Evolution in Aqueous Solution. *Inorg. Chem.* **1999**, *38*, 5086–5090. [CrossRef] [PubMed]
26. Yuan, X.R.; Song, C.; Wang, H.; Zhang, J. *Electrochemical Impedance Spectroscopy in PEM Fuel Cells: Fundamentals and Applications*; Springer: Berlin/Heidelberg, Germany, 2010.
27. Gidi, L.; Honores, J.; Ibarra, J.; Arce, R.; Aguirre, M.J.; Ramírez, G. Improved photoelectrocatalytic effect of Co (ii) and Fe (iii) mixed porphyrins on graphite paste electrodes towards hydrogen evolution reaction. *New J. Chem.* **2019**, *43*, 12727–12733. [CrossRef]
28. Voiry, D.; Yamaguchi, H.; Li, J.; Silva, R.; Alves, D.C.B.; Fujita, T.; Chen, M.; Asefa, T.; Shenoy, V.B.; Eda, G.; et al. Enhanced catalytic activity in strained chemically exfoliated WS 2 nanosheets for hydrogen evolution. *Nat. Mater.* **2013**, *12*, 850–855. [CrossRef] [PubMed]
29. Văduva, C.C.; Vaszilcsin, N.; Kellenberger, A.; Medeleanu, M. Catalytic enhancement of hydrogen evolution reaction on copper in the presence of benzylamine. *Int. J. Hydrog. Energy* **2011**, *36*, 6994–7001. [CrossRef]
30. Ramírez, G.; Lucero, M.; Riquelme, A.; Villagrán, M.; Costamagna, J.; Trollund, E.; Aguirre, M.J. A supramolecular cobalt–porphyrin-modified electrode, toward the electroreduction of CO_2. *J. Coord. Chem.* **2004**, *57*, 249–255. [CrossRef]
31. Pentland, N.; Bockris, J.M.; Sheldon, E. Hydrogen evolution reaction on copper, gold, molybdenum, palladium, rhodium, and iron mechanism and measurement technique under high purity conditions. *J. Electrochem. Soc.* **1957**, *104*, 182–194. [CrossRef]
32. Zeng, K.; Zhang, D. Recent progress in alkaline water electrolysis for hydrogen production and applications. *Prog. Energy Combust. Sci.* **2010**, *36*, 307–326. [CrossRef]
33. Muthukumar, P.; Moon, D.; Anthony, S.P. Copper coordination polymer electrocatalyst for strong hydrogen evolution reaction activity in neutral medium: Influence of coordination environment and network structure. *Catal. Sci. Technol.* **2019**, *9*, 4347–4354. [CrossRef]
34. Beyene, B.B.; Mane, S.B.; Hung, C.-H. Electrochemical Hydrogen Evolution by Cobalt (II) Porphyrins: Effects of Ligand Modification on Catalytic Activity, Efficiency and Overpotentia. *J. Electrochem. Soc.* **2018**, *165*, H481–H487. [CrossRef]
35. Khnayzer, R.S.; Thoi, V.S.; Nippe, M.; King, A.E.; Jurss, J.W.; el Roz, K.A.; Long, J.R.; Chang, C.J.; Castellano, F.N. towards a Comprehensive Understanding of Visible-Light Photogeneration of Hydrogen from Water Using Cobalt (II) Polypyridyl Catalysts. *Energy Environ. Sci.* **2014**, *7*, 1477–1488. [CrossRef]
36. Fu, L.-Z.; Zhou, L.L.; Tang, L.Z.; Zhang, Y.X.; Zhan, S.Z. Electrochemical and photochemical-driven hydrogen evolution catalyzed by a dinuclear cobalt (II)–triazenido complex with high turnover number. *Int. J. Hydrog. Energy* **2015**, *40*, 5099–5105.
37. Domańska, U.; Skiba, K.; Zawadzki, M.; Paduszyński, K.; Królikowski, M. Synthesis, physical, and thermodynamic properties of 1-alkyl-cyanopyridinium bis {(trifluoromethyl) sulfonyl} imide ionic liquids. *J. Chem. Thermodyn.* **2013**, *56*, 153–161. [CrossRef]